Heliyon 10 (2024) e33641

Contents lists available at ScienceDirect

Heliyon

journal homepage: www.cell.com/heliyon

Research article

# Characterization of *Calotropis gigantiea* plant leaves biomass-based bioplasticizers for biofilm applications

Shanmuga Sundari Chandraraj [a], Indran Suyambulingam [b], Naushad Edayadulla [a], Divya Divakaran [b], Manoj Kumar Singh [b,*], M.R. Sanjay [b], Suchart Siengchin [b]

[a] *Department of Chemistry, Vel Tech Rangarajan Dr. Sagunthala R&D Institute of Science and Technology, Chennai, 600062, India*
[b] *Natural Composites Research Group Lab, Department of Materials and Production Engineering, The Sirindhorn International Thai-German School of Engineering (TGGS), King Mongkut's University of Technology North Bangkok (KMUTNB), Bangkok, 10800, Thailand*

ARTICLE INFO

*Keywords:*
*Calotropis gigantiea*
Bioplasticizer
Biofilm
Biofiller
Biomaterial
Biomass valorization

ABSTRACT

The present surge in environmental consciousness has pushed for the use of biodegradable plasticizers, which are sustainable and abundant in plant resources. As a result of their biocompatibility and biodegradability, *Calotropis gigantiea* leaf plasticizers (CLP) serve as viable alternatives to chemical plasticizers. First time, the natural plasticizers from the Calotropis leaves were extracted for this study using a suitable chemical approach that was also environmentally friendly. The XRD results showed a reduced crystallinity index of 20.2 % and a crystalline size of 5.3 nm, respectively. TGA study revealed that the CLP has good thermal stability (244 °C). Through FT-IR study, the existence of organic compounds in CLP can be investigated by key functional groups such as alcohol, amine, amide, hydrocarbon, alkene, aromatic, etc. Further the presence of alcoholic, amino, and carboxyl constituents was confirmed by UV investigation. SEM, EDAX analysis, and AFM are used to examine the surface morphology of the isolated plasticizer. SEM pictures reveal rough surfaces on the CLP surface pores, which makes them suitable for plasticizing new bioplastics with improved mechanical properties. Poly (butylene adipate-co-terephthalate) (PBAT), a biodegradable polymer matrix, was used to investigate the plasticization impact after the macromolecules were characterised. The biofilm PBAT/CLP had a thickness of 0.8 mm. In addition, the reinforcement interface was examined using scanning electron microscopy. When CLP is loaded differently in PBAT, the tensile strength and young modulus change from 15.30 to 24.60 MPa and from 137 to 168 MPa, respectively. CLP-reinforced films demonstrated better surface compatibility and enhanced flexibility at a loading of 2 % when compared to pure PBAT films. Considering several documented characteristics, CLP may prove to be an excellent plasticizer for resolving environmental issues in the future.

## 1. Introduction

Polymers made from biomass are composed of substances that come from renewable resources. Due to the necessity and desire for alternatives to polymers based on fossil fuels, their biodegradable qualities have drawn attention from academics and manufacturers worldwide in recent years. The industry is made sustainable by the usage of biodegradable polymers [1,2]. The majority of the raw

* Corresponding author.
*E-mail addresses:* indransdesign@gmail.com (I. Suyambulingam), manojsingh.iitmandi@gmail.com (M.K. Singh).

https://doi.org/10.1016/j.heliyon.2024.e33641
Received 23 February 2024; Received in revised form 24 June 2024; Accepted 25 June 2024
Available online 26 June 2024

ingredients used to create synthetic polymers from petrochemicals, on the other hand, are not biodegradable and will ultimately run out. Bio-mass polymers comprises a very small percentage of the global plastic business, notwithstanding these benefits [3]. The challenges associated with the non-biodegradability of synthetic pharmaceutical inactive components have driven developers to focus on the creation of biopolymers. Natural biodegradable excipients have drawn a lot of interest now because of their designed uses and sustainability [4,5]. Key components of its sustainable development are innovative graft-polymerization or co-processing processes that convert raw resources into value-added compounds by fabricating high-performance, multifunctional, low-cost polymers with customisable structures [6].

Biopolymers have limited potential for usage in a variety of packaging applications because to their fragility and brittleness during thermo-formation, which results in poor mechanical qualities regarding process-ability and end-use application. Utilising different kinds of plasticizers has become more popular recently as a way to get around this drawback of biopolymers [7–9]. Low molecular weight, relatively stable organic combinations known as plasticizers are a family of chemicals that help diminish the rigidity of the polymer's three-dimensional structure and increase its capacity to break down without breaking by reducing the amount of contact between the molecules. This increases the workability and durability of polymers [10]. Plasticizers are used in the manufacturing process and/or during subsequent usage to increase the flexibility and pliability of plastics. Commonly used industrial plasticizers, like phthalates, are scrutinised, nevertheless, as some of them may be hazardous to human health or the environment. Because of this, alternatives are being looked for globally that may be manufactured preferably from renewable raw resources and give at least equal quality at reasonable rates [11].

Generally, plasticizers have the potential to seep out of many items, into food, and into the environment. In this manner, they can be consumed in large quantities through a daily diet. Significant sources of plasticizers in indoor air and household dust include building materials like electrical cables, floor coverings, handrails, door and window seals, furniture made with phthalate-containing adhesives or paints, home furnishings, bath and shower inlays and shower curtains. Customers should aim to steer clear of plastics that include flexibilizers as much as possible, especially soft PVC, and instead choose other goods. In view of this, there is a growing trend in the application of natural plasticizers., particularly epoxidized triglyceride vegetable oils extracted from sunflower [12], castor [13], and soybean oils [14]. These oils have low toxicity and low migration. The habitat of several wild creatures is destroyed during the process of extracting that oil, which frequently entails chopping down trees and excavating the earth. Further linking the hunt for natural plasticizers to the growing interest of industry and material scientists in creating novel bio-based products produced using biodegradable and renewable resources that could cut down on the usage of traditional plastic products. Plasticizers for biopolymers need to ideally also be biodegradable, which seems reasonable to assume. Garbage wastes, farming leftovers, and discarded biomass are the usual birthplaces of bio-plasticizers. Plants are the primary source of biopolymers and bio-plasticizers since they may produce a variety of secondary metabolites through various metabolic processes. For example, a range of saccharide derivatives and sugars that can be used as plasticizers may be produced from the starches and cellulose found in plants like potatoes, maize and wheat (fructose, mannose, glucose, sorbitol, mannitol, xylitol) [15]. A wide range of citrates & itaconates, that are produced from sugar cane [16] or else citrus fruits also used as plasticizers [17], have citric acid as a highly desired precursor. Studies have been conducted on lecithin, waxes, and other substances, such as amino acids, as potential plasticizers for films [18] that are edible or biodegradable.

*Calotropis gigantiea* (*C. gigantiea*) (L.) R.Br, belongs to Apocynaceae family often referred to as "badabadam" or "erruku" in local dialect, is native to Asia and Africa and is extensively accessible across India [19]. It is a hardy, upright, woolly shrub with many branches that can withstand droughts. It may be cultivated up to 900 m above sea level in all climate zones. The soft stem is composed of a white waxy or powdery pubescence, smooth-surfaced rectangular leaves with a cottony base, and obovate leaves and a mature, round, woody stem. The seeds are brown, wide, oval, measuring around 2.5–3.2 cm, with the pointy end has a white, silky hair tuft. The blooms are often purple, white, or lilac in colour and appear in complicated to simple cymose-corymbs. Although *C. gigantiea* is mostly found in wastelands, it has been used widely in India since the 10th century for a variety of ailments [20]. Reports from the digital collection of traditional knowledge make it evident that it has been used in Indian medical practices, such as Ayurveda, Siddha, and Unani formulations. Along with other plants and minerals, Plant materials such as freshly picked leaves, flowers, their roots, root bark, and concentrated juice were often used in the formulations. Numerous phytochemicals were extracted from *C.* gigantiea, which became physiologically active [21]. The investigation of renewable, conveniently available, environmentally benign, and biodegradable bio-plasticizers reduces the negative aspects associated with synthetic plasticizers.

Following up on our curiosity, we have extracted the natural plasticizers from the *C. gigantiea* leaves using a suitable environmentally friendly chemical approach. For the first time, the physico-chemical, thermal as well as microstructural characteristics of novel CLP plasticizers were examined. We used a matrix called polybutylene adipate terephthalate (PBAT) to generate biofilm for innovative applications, and we appraised the effect of these bioplasticizers on plasticizing. The appropriateness of the manufactured films for packaging applications was further assessed by suitable analysis.

## 2. Materials and methodology

### 2.1. Materials

The *C.gigantiea* (L.) R.Br plant leaves was collected from the waste lands in Kanyakumari district, Tamilnadu, India. To get rid of dust, the leaves were thoroughly washed in clean water. The fresh leaves were then finely cut into small pieces and subjected to further treatment process. All the chemicals used in the analysis were analytical grade purchased from Sigma-Aldrich, India.

### 2.2. Extraction method of plasticizer

After being chopped, the 200 g of chopped *C. gigantiea* leaves are added to the mixture of 20 ml of 0.1 N HCl and 2 g KCl in 200 ml of water and it was agitated with a magnetic stirrer at room temperature (slow pyrolysis). After that the mixture was exposed to surface catalysis by adding 4–5 ml of benzoalkonium chloride. Then 50 ml of 10 % ammonia.and Dimethyl formamide was added gradually, mixed well for 20 min, and then allowed to soak for 4 h. The hydrocolloids and organic soluble phenolic are dispersed throughout the mixture. The mixture was then separated and filtered. The collected colloidal mixture was then vacuum-dried for 6 h at 80 °C [22]. The plasticizer was used for further analysis once it had solidified and been powdered. (Fig. 1).

### 2.3. Preparation of biofilm

Solution casting method was used to fabricate the plasticizer from *C. gigantiea* leaves (CLP) and the polybutylene adipate-*co*-terephthalate (PBAT) film. The plasticizer is taken into account while weighing the PBAT for each composition. For 1 h, the PBAT (0.95 g in 10 ml chloroform) and the powdered *C. gigantiea* leaves (CLP of 0.05 g) plasticizer were combined in a magnetic stirrer. Subsequently, pure PBAT (control) and-PBAT/2 % CLP films were fabricated using solvent casting method. For that, the required quantity of CLP filler was added to the PBAT solution and assorted well using a magnetic stirrer for 1 h, to obtain a homogenous solution. In case of control, pure PBAT film was prepared without CLP. The resultant viscous solution was casted into petri plate (150mm × 50 mm) and permitted to dry in a desiccator at ambient temperature for 12 h. The obtained films were detached from the petri plates and subjected for various testing.

## 3. Characterization of plasticizer

In accordance with standard profile, the separated bioplasticizers' physico-chemical, thermal, and surface features were examined to determine the uniqueness of the bioplasticizer. In order to figure out the material's specific density and determine if it is suitable for use as a bio-plasticizer in lightweight applications, physical examination of the material is required. Crystallinity, functional groups, and principal chemical composition of the substance were all ascertained with the use of the chemical analysis. To determine the surface properties and temperature endurance of the extracted biopolymers, thermal tests and surface morphological analysis were performed. This allowed for the determination of the biopolymers' appropriateness for the creation of composites or biofilms.

### 3.1. Fourier transform infrared spectroscopy

IR spectra were acquired in KBr using a Jasco 4600 Fourier transform infrared spectrophotometer in order to decide the various functional groups that are existing in the CLP. The study was conducted using a 4 cm-1 resolution in non-contact mode. After that, the

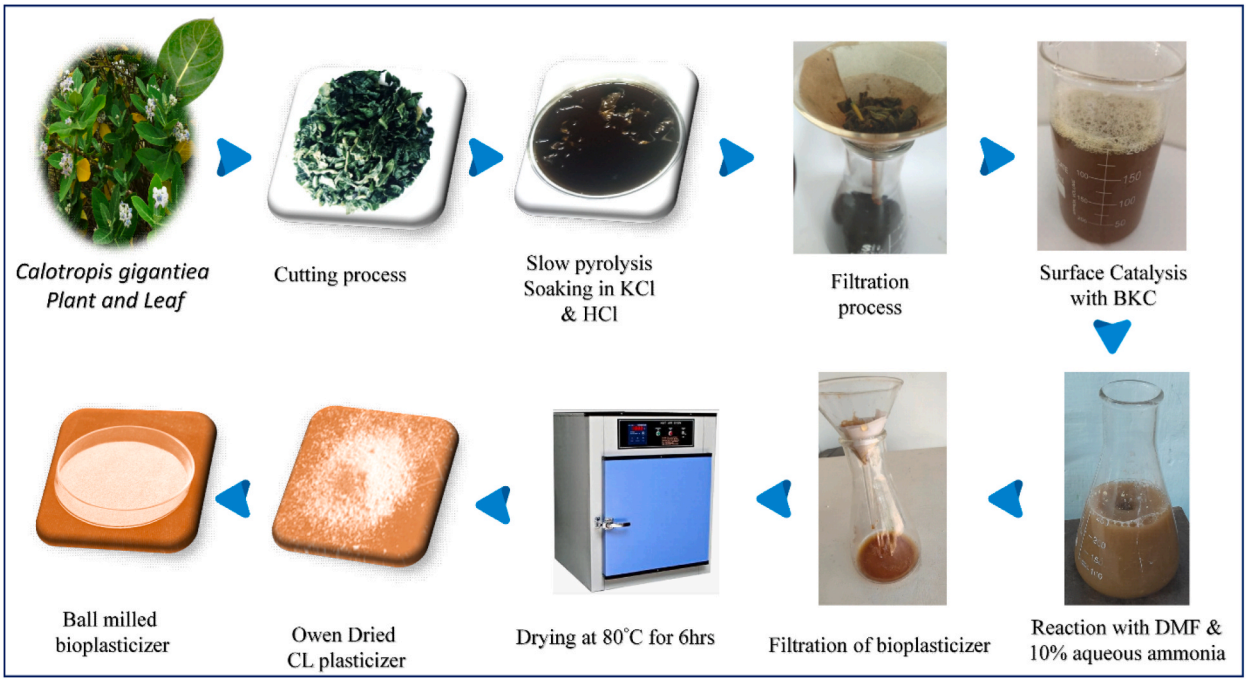


**Fig. 1.** Extraction process of plasticizer based on *Calotropis gigantiea* leaves.

4000-500 $cm^{-1}$ wavelength range FT-IR spectra were obtained at ambient temperature. The generated spectrogram was also used to elucidate the chemical groups [23] and connected chemical constituents that were existing in the suspected substance, as well as to validate its chemical makeup and plasticizing characteristics.

### 3.2. UV spectroscopy analysis

The sample was fed into an integrating sphere on a Shimadzu UV-2101 PC spectrometer, which was used to perform a UV visible spectroscopic analysis of the separated bioplasticizer. The resulting visible spectrum was measured between 200 and 700 nm in wavelength. The existence of compounds with plasticizing abilities is confirmed by the unique peaks observed in the spectrum [24].

### 3.3. X-ray diffraction investigation

The XRD performance was utilised to ascertain the % of crystalline plus amorphous fractions present in the CLP. This experiment was conducted using apparatus from the Bruker XRD series. After placing the extracted CLP in the sample holder, the holder was placed under an X-ray machine. The voltage and current settings for the X-ray generator were set at 30.0 kV and 10.0 mA, respectively. After that, X-rays of 1.54060A∘ were shielded on the material, and the diffracted X-rays were detected at a scanning rate of 0.020°/80 s while the detector was moved from 2θ = 20°–80°. The system was maintained at 25 °C [25]. The Origin Pro 2021 programme was utilised to calculate the crystallite size (CS) & crystallinity index (CI) of the bioplasticizer by using equations (1) and (2). In reference (1), $A_{crystalline}$ denotes the crystalline curve percentage, whereas $A_{amorphous}$ denotes the amorphous curve fraction. Scherrer's equation is represented by the symbol $\lambda$, the particular wavelength is denoted by β (Bragg's angle; CUKα = 1.5406 Å), which is the full-width at half-maximum wavelength of a line change, and D (crystallinity size) is the wavelength.

$$\mathrm{CI}(\%) = \frac{A_{\mathrm{crystalline}}}{A_{\mathrm{crystalline}} + A_{\mathrm{amorphous}}} * 100 \tag{1}$$

$$D = \frac{\mathrm{k}\lambda}{\beta \cos\theta} \tag{2}$$

### 3.4. Thermal analysis

#### 3.4.1. Thermo gravimeteric analysis (TGA) of CLP

A thermogravimetric analysis (TGA) was performed on the CLP using a TG/DTA Exstar 6300 apparatus. The heat and hydration deficit properties of CLP are essential for the improvement of bioplasticizers intended for extreme temperatures and high-efficiency applications. The CLP can also be used as a binding substance in polymers. Here, TGA was employed to investigate the CLP's heat steadiness and degrading qualities. The analysis was conducted in an environment containing nitrogen. Before the CLP sample (4.5 mg) was positioned in an alumina furnace that was heated to room temperature, it was weighed. At a constant pace of 20 °C per minute, the sample's temperature rose from 30 °C to 900 °C. TGA graphs displayed the amount of weight loss (%) in relation to temperature. The CLP sample was subjected to differential thermographic (DTG) analysis, which used the peaks created to ascertain the sample's breakdown at particular temperatures. The highest temperature of deterioration threshold for the recommended plasticizer was estimated using the TGA along with DTG plots.

#### 3.4.2. Activation energy study

Coats–Redfern method used to determine the kinetic parameters of solid-state materials with non-isothermal model fitting. The Coats-Redfern formula (Equation (3)) below was implemented to do a kinetic energy assessment of the CLP.

$$\ln\left[\frac{g(x)}{T^2}\right] = ln\left[\frac{AR}{\beta E}\left(1 - \frac{2RT}{E}\right)\right] - \frac{E}{R}\frac{1}{T} \tag{3}$$

In this case, the integral version of the reaction dt/dx mechanism model is denoted as g (x)., t stands for time (min), for linear heating rate, T stands for Kelvin absolute temperature, and R represents the universal gas constant, that is 8.314 J $mol^{-1}$ $K^{-1}$.

### 3.5. AFM analysis

The Flex AFM 5 instrument was used to get measurements from the CLP sample's surface. The scanner head on the apparatus has a resolution of 0.1 nm. The information is fed back into the algorithm once more to generate topographical features. A nanoscale AFM was used to measure the roughness profile's total height (Rt), the surface average roughness (Ra), space within the surface's tallest 'peak' and deepest 'valley' (Rz), and root mean square deviation value of the profile's deviations from the mean line (Rq/Rrms) [26]. By dividing the fourth power of Rq inside the sample length (Rku) by the mean of the height values, the sharpness of the surface height distribution was determined. High kurtosis values are associated with spiky surfaces, whereas low kurtosis values are associated with bumpy surfaces. The surface's departure from symmetry, or skewness (Rsk), is calculated as the mean of the surface's first derivative.

### 3.6. Scanning electron microscopy study

The surface microstructure of the obtained CLP sample was inspected via SEM analysis utilising the Σ version of Carl Zeiss, Germany, 5.07 Beta - Field Emission Scanning Electron Microscope (FESEM). In this investigation, the voltage amplification was fixed to 15 kV, and the operating distance of about 12.2 mm was chosen. The photographs have been adjusted for brightness and contrast such that the particles could be distinguished from the backdrop. Two photos total, each at a different magnification of 200× and 2000 ×. For the particle size investigation, 21 particles were studied using the ImageJ image-processing programme from the National Institutes of Health, so as to ascertain the shape and mean length (m) characteristics. Thermo ScientificTM AxiaTM ChemiSEMTM Scanning Electron Microscope was used to conduct interfacial bonding investigations and evaluate the impact of plasticizer on PLA-based biofilms.

### 3.7. EDX spectroscopy analysis

It is possible to accurately measure the elements (such as oxygen, carbon, magnesium, nitrogen, sodium, etc.) present on the extracted CLP by employing energy dispersive X-ray spectrophotometer (EDX). Five measurements were made of the element distributions for the treated materials using an INCAPenta FETx3 model EDX analyzer and a TESCON VEGA (third generation) scanning electron microscope. After then, the mean value was calculated.

### 3.8. Particle size analysis

The imaging programme "ImageJ" was performed to investigate the plasticizer particles seen in the SEM picture. This programme was utilised to analyse the particles found in different locations utilising minimum points from 21 samples, and it was then utilised to tabulate the data.

## 4. Results and discussion

### 4.1. Fourier transform infrared spectroscopy (FT-IR)

The FT-IR spectrum is essential for plasticizer synthesis because it may be used to identify functional groups that possess certain properties. FT-IR was used to study the CLP plasticizer, as seen in Fig. 2. Strong broad bands in the 3700–3000 $cm^{-1}$ range are typically attributed to O–H or N–H stretching. These functional groups are present in proteins, polysaccharides, flavonoids and adsorbed water. The medium sharp peak at 2921 $cm^{-1}$ is attributed to asymmetric C–H stretching in $sp^2$ hybridised carbon. This provides details on the presence of unsaturated –CH = bonding. As a result of the aromatic methoxyl, methyl, and methylene groups' CH stretching vibration, Fig. 3 shows two distinct, strongly absorbed peaks, one symmetrically at 2921 $cm^{-1}$ and the other asymmetrically at 2854 $cm^{-1}$. The linear stretch of alkene groups could be connected to this stretching. Methoxy stretching can be accredited to the peak at 2854.09 $cm^{-1}$. This methoxy group can be connected to a linear chain or an aromatic ring. The peak located at 1635.54 $cm^{-1}$ indicates the existence of frequency regarding carbonyl stretching of flavonoids and lipids in the sample material. Additionally, the water's H–*O*–H bending is seen at 1620 $cm^{-1}$ and 1642 $cm^{-1}$; if not, one possible explanation could be either alkyne stretching or C═C conjugate stretching of aliphatic group. The bands at 1635.54 $cm^{-1}$ may have been found due to vibrations in the flavonoids and lipids' C═O groups as well as their C═C groups, which may be made up of cyclic structures connected by a ring resonance that enhances stability.

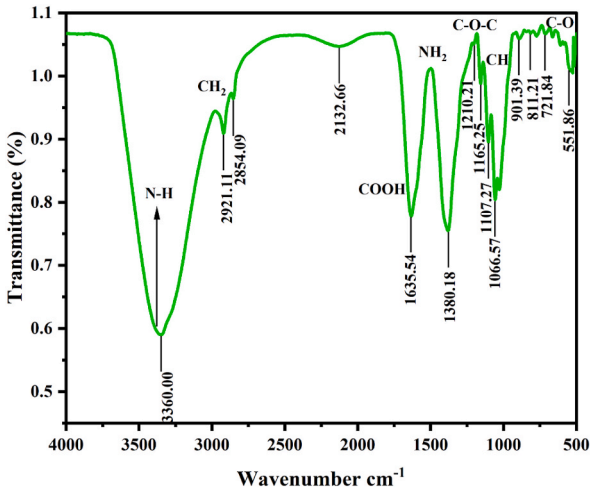


**Fig. 2.** FT-IR spectroscopy of the CLP.

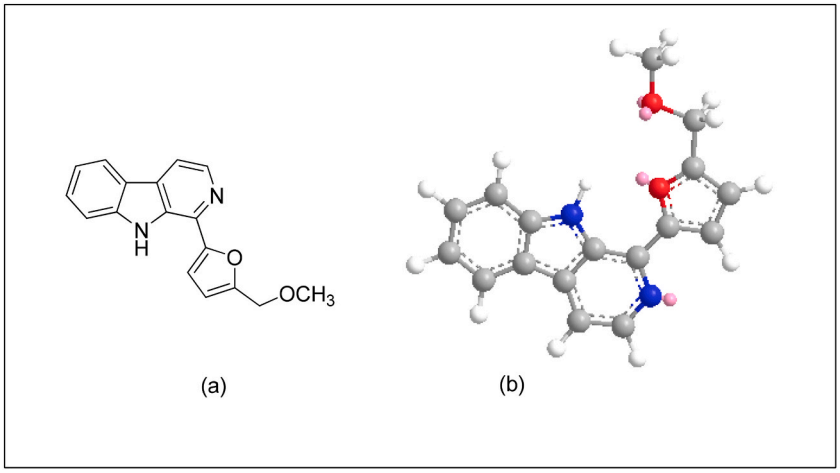


**Fig. 3.** (a&b). Proposed chemical structure of CLP biomass (a) 3D view (b).

The material's existence of alkenes, conjugated ketone, organic nitriles, and open-chain imino or azo group is confirmed by a sharp stretching vibration at 1635.54 $cm^{-1}$. The delignification procedure has removed the ester group carbonyl vibrations from the lignin components' feruloyl, acetyl, and *p*-coumaryl groups, as seen by the signal at 1739 $cm^{-1}$ being absent. The biomass's CH–bending and $CH_3$ stretch are attributed to the peak at 1380.18 $cm^{-1}$. The existence of –C–O–C– stretching is responsible for the finger print region's peak at 1210.21 $cm^{-1}$ which ascribed owed to the existence of glycosidic groups. Zhang et al. state that in the range of 1145–1025 $cm^{-1}$, (C–O–C) glycosidic bend vibrations and the (C–OH) side group stretching vibrations are observed for the presence of polysaccharides and oligosaccharides. With the functional group C–Cl, the peak at 811.21 $cm^{-1}$ illustrates a little contaminant brought about by bleaching in the sample (Table 1). Proposed chemical structure of CLP biomass (a) 3D view (b) were depicted in Fig. 3a and b.

### 4.2. *UV–visible absorption spectra study of CLP*

The obtained spectral datas are displayed in Fig. 4, which show the absorption of UV light inbetween 200 nm and 700 nm in wavelength of the bioplasticizer sample. In the absorbance range of 200–400 nm, bioactive chemicals such as flavonoids and other polyphenolic compounds are present. In actuality, transparency is dependent on the size or kind of material; it is employed to describe structural dimensions [27]. In the UV absorption range (180–280 nm), there aren't many peaks associated with CLP.Formerly detected small peaks at 210–230 nm demonstrates the hydroxyl groups' presence (ethanol, methanol, phenol, etc.). The similar pattern was seen

**Table 1**
Absorption range of different functional groups present in CLP.

| Sl. No. | Observed peak values ($cm^{-1}$) | Chemical composition | Functional group |
|---|---|---|---|
| 1 | 3360 | Strong wide stretch (O–H or N–H) | Alcohols, amines, amides, and Phenols |
| 2 | 2921.11 | Medium (C–H stretching of methylene) varying wide stretch (O–H) | Alkanes carboxylic acids |
| 3 | 2854.09 | Asymmetric CH stretching<br>$O–CH_3$ | Hydrocarbons<br>Methoxy |
| 4 | 2132.66 | Weak stretch<br>C ≡C | Alkynes |
| 5 | 1635.54 | Medium C═C stretch<br>Medium C–C stretch<br>C═O stretching<br>Bending vibrational frequency of N–H | Alkenes<br>Aromatics<br>Carboxylic acid<br>Amines |
| 6 | 1380.18 | Strong CH bending | Alkanes |
| 7 | 1210.21 | C–*O*–C | Glycosidic group |
| 8 | 1165.25 | C–N stretching | Primary amines |
| 9 | 1107.27 | Stretching and bending modes of (C–OH) & C–*O*–C | Polysaccharides & oligosaccharides |
| 10 | 1066.57 | Strong stretch<br>C–O ($O–CH_3$)<br>Variable stretch C–N | Esters, ethers, alcohols, methoxy, carboxylic acids<br>Aliphatic Amines |
| 11 | 901.39 | N–H wagging | Primary/Secondary Amines |
| 12 | 811.21 | C–Cl | Halogens |
| 13 | 721.84 | *cis* = C–H out-of-plane bending | |
| 14 | 551.86 | C–O | Alkoxy |

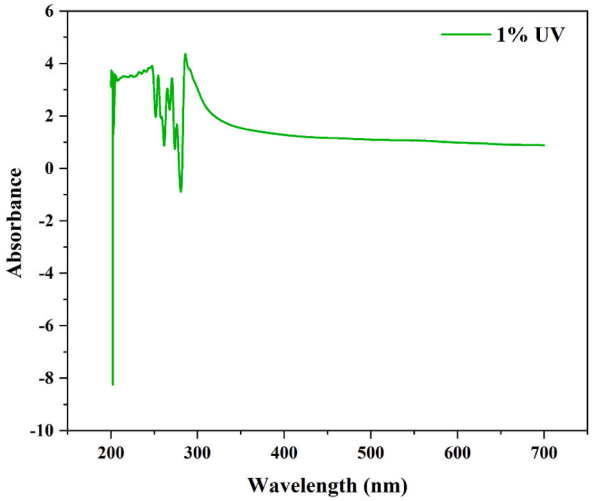


**Fig. 4.** UV–visible spectroscopy of the CLP macromolecules.

in earlier research, which suggested that common chemical moieties including methyl, carboxyl, hydroxyl, and amino groups (C═O, –COOH, –COOR, or –$CONH_2$) are responsible for the shorter wavelengths' (200–250 nm) and low absorption peak. Similarly, the corresponding signal seen at 280 nm indicates the presence of a carbonyl group. According to another study, the carbonyl group is identified by the peak in between 186 and 280 nm. Analogous chemically sensitive groups were also detected in the FT-IR spectra, which also showed the existence of carbonyl, methyl, hydroxyl, and carboxyl groups [28].

### *4.3. XRD diffractogram depicted the crystalline characteristics of CLP*

Fig. 5 displays the obtained x-ray diffractograms for CLP in the 2θ array of 20°–80°. Low intensity observations of the distinctive sharp peak were made at approximately 45.43°. Several less intense peaks, such as 22.49°, 31.89°, 54.52°, and 75.95°, were also seen at varying 2θ values inside this signature peak. The degree of crystallinity and peak height are directly correlated. A plasticizer is discovered to consist of both crystalline and amorphous areas based on the acquired diffraction pattern. It is noted that there are several broad peaks and one sharp peak at approximately 2θ = 45.43°. The PVA–MgTf–50 sample of weight % EC system primarily exhibits the broadest peak because it has the highest amorphous area [29]. Similar specific peaks (22.17°, 31.73°, 45.58°, 56.81°, and 75.43°) were observed for the bio-plasticizers derived from *Nelumbo nucifera* leaf [30].

The semi-crystalline structure of the CLP is revealed by the mixing of crystalline and amorphous peaks. But the peak's extremely low intensity indicates that it belongs to the more amorphous nature. The quality of crystallinity was calculated in order to look into the percentage of crystalline/amorphous material in the CLP in more detail. It was discovered that the CLP had a crystallite size of 5.3 nm & a crystallinity index (CI) of 20.2 %. Previous research has shown that a high value of amorphous nature is indicated by a low CI value [31,32]. Based on XRD data, it can be concluded that sample CLP has the maximum degree of amorphous nature. Furthermore, the weak crystallinity index and crystalline size are mandatory to offer the plasticizing action that increases the substance's flexibility,

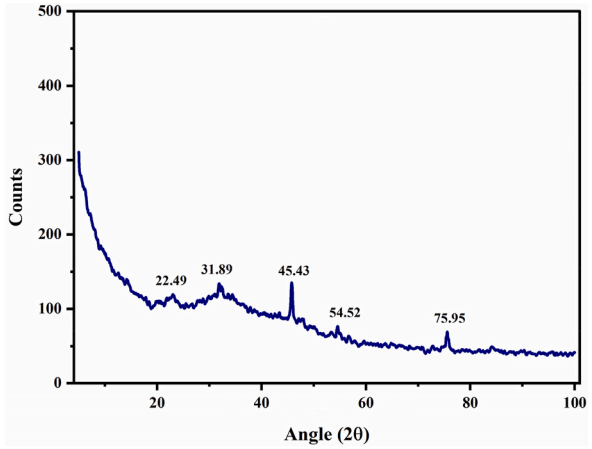


**Fig. 5.** The XRD spectra of bioplasticizer obtained from *C. gigantiea* leaves.

compatibility, and frequently allows simple incorporation into polymer matrix possible [33]. The crystallinity of biodegradable polymers affects their biodegradability and significantly affects their physical properties, including their tensile and thermal capacities. These findings concur with those that have been previously published [34]. The results also agreed that the reason for the lack of an ordered crystalline peak was that the bioplasticizer that was formed was mostly composed of organic materials, with no inorganic deposits developing.

### 4.4. Thermal analysis

#### 4.4.1. Thermo gravimeteric analysis (TGA) of CLP

When it comes to the industrial and scientific viewpoints on the development of biocomposites, TGA is a vital analysis tool for observing the degradation and thermal behaviour of bioplasticizers. When heat was applied to the bioplasticizer, the bioplasticizer's weight was seen to decrease with temperature.

The heat steadiness of a polymeric sample is determined by intrinsic properties of macromolecules along with molecular connections between different molecules. Specific chemical bonds, or the chains of macromolecules, will break when the heat energy given exceeds their bond dissociation energy [35]. The TG & DTG of the samples of CLP are presented in Fig. 6a. The temperature at which noticeable weight loss occurs can be found using the DTG curves. The thermal deterioration and mass loss of the CLP appeared to occur in three separate phases, each of which was associated with a DTG curve peak that stood for a particular heating event. It appeared that all of the curves followed a similar trend. The result showed how strong the bioplasticizer was in relation to heat. The initial loss of mass was produced by a thermal action that took place at temperatures lower than 100 °C. This activity was primarily responsible for the evaporation of around 32 % of the moisture and water fragments. The process of thermal breakdown caused by water evaporation occurs, and the loss of very light volatile matter [36]. Simultaneously, this phase was associated with mass loss, which can be clarified by the dissolution of low molecular mass molecules and weak interactions between water molecules [37]. Because of their greater hydrophilicity, which is compatible with their high percentage of water, CLP showed larger percentages of weight loss during this stage [38]. As seen in Fig. 6a, the mass did not decrease between 100 °C and 200 °C. The second stage of CLP's thermal deterioration occurred between 200 °C and 250 °C, resulting in a 15 % weight loss. The volatilization of bio-based plasticizer molecules along with volatile matter was primarily liable for this mass loss. Researchers have previously reported similar findings [39]. The haphazard breakage of the glycosidic bond and the disintegration of hemicellulose indicate this stage. Levoglucosan is created when the glucose ring's hydroxyl group becomes dehydrated. Next, when the glucose ring is broken, the aldehyde group is formed. Furans having $–CH_2$ or $–CH_2$-*O*-$CH_2$ as the main chain and aromatic rings like benzene substitutes are formed when the temperature rises [40].

Stage 3 is the stage that occurs when the samples at temperatures ranging from 250 °C to 900 °C release volatile substances. At 300 °C, lignin starts to degrade. It is extensively cross-linked, has three distinct types of benzene-propane units, and has a very high molecular weight. Thus, lignin is difficult to break down and has a very high heat stability [41]. The charcoal becomes flammable at this moment due to the volatile materials surrounding it and the surface has been exposed to oxygen, which simultaneously burns the volatile stuff and the charcoal. This step follows the emission of volatile materials that either emit or create carbon [42]. As both chain breaking and cyclization are involved in the thermal degradation of polyenes, the crosslinking of molecules with C═C bonds is assumed to occur beyond 400 °C [43]. This step of the carbonisation process, which starts at temperatures above 500 °C, was indicated by raising the aromatic carbon resonance's intensity and lowering the aliphatic carbon resonance's intensity [40]. The leftover residue samples contained inorganic components that were created when carbonated compounds were pyrolyzed at temperatures above 500 °C [44]. The successive heat transfer damaged the substance's comparatively heat-stable components, including saponins, tannins,

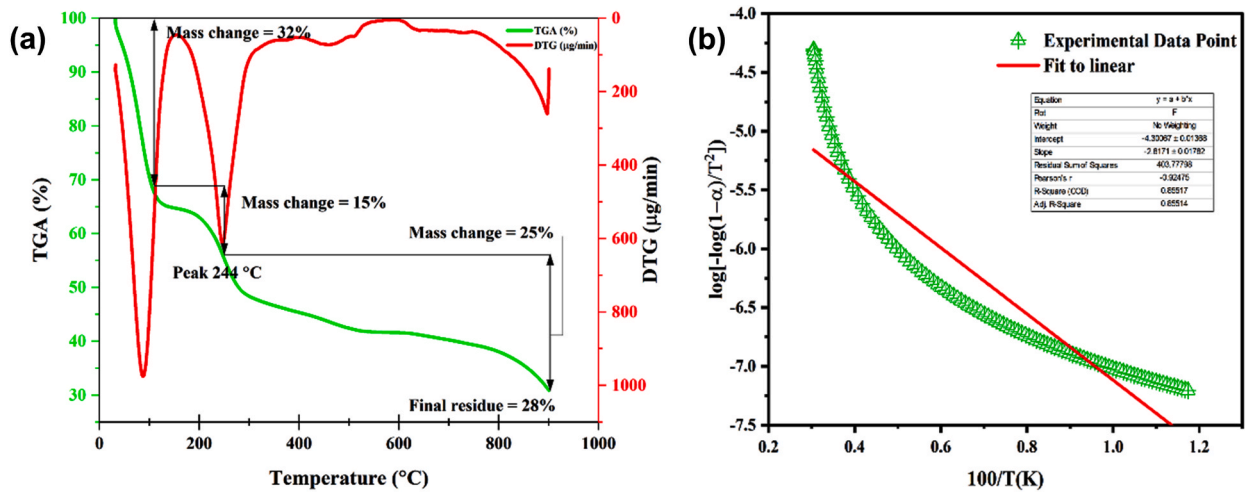


**Fig. 6.** TGA/DTG curves and (b) Coats-Redfern plot of CLP.

with other non-ferrous elements. The last stage of deterioration was this. There was only 28 % of the initial residue remaining. The third notable weight reduction was brought on by the char residue oxidation [22,45]. The weight loss increased with temperature, as shown by the TGA in Fig. 6a, and the DTG curve showed that the maximum deterioration occurred at 244 °C. Without a doubt, the DTG curve supports the TGA pattern. At 244 °C, dehydration, depolymerization, and breakdown of hydroxyl units resulted in the degradation of CLP, which is explained by the char's oxidation and decomposition into low-molecular-weight volatile molecules. Char was then produced [46]. Similar thermal studies for a variety of biopolymers were also shown, including Plasticizer made from waste using repurposed modified palm oil to produce non-glutinous thermoplastic starch foam is 290 °C [37], $T_{max}$ at 321.53 °C, is shown in films with arrowroot starch (AS) and glycerol (G) which acting as plasticizer [47]. Based on thiophene with ricinoleic acid, a triester-amide is a primary plasticizer for PVC shows the breaks down between 311.83 and 413.83 °C [48]. Thermal disintegrate of fire-resistant bio-based co-plasticizer for PVC synthetic compounds arises at 300.2 °C [49], As bio-based plasticizers (epoxidized esters of glycerol generated from soybean and canola oil) are examined with natural rubber, the plasticizer along with all other low-molecular components decompose at 350 °C [46]. Because of its limited thermal stability, which firmly proved its amorphous nature, our current work, in comparison, displays a low $T_{max}$ value.

#### 4.4.2. Kinetic analysis

Based on the TGA information, the kinetic energy was determined using the Coats-Redfern method (Fig. 6b), where all variables were covered by a single line. The slope of the straight line can be used to compute the active energy (E). It was determined that the activation energy (E) was approximately 53.98 kJ $mol^{-1}$. Reaction rate will drop because it will be harder to start the reaction process with a higher activation energy. The low activation energy demonstrates the weak bonds that exist between volatile chemicals and biomolecules.

### 4.5. Surface roughness study using AFM

AFM imaging allowed a smaller-scale description of the microstructure of the CLP. To get the photos, topographical contrast was used. This technique has been engaged to furnish both qualitative as well as quantitative data regarding biomolecules at the nanoscale, which is sometimes unavailable through other means of experimentation. For surface study, the AFM technique is a powerful tool. CLP's AFM images with a surface in two and three dimensions are shown in Fig. 7 (a & c). The region in Fig. 7c is scattered with several pointy peaks and deeper valleys. Using AFM, the morphology and roughness of the plasticizer were investigated. Fig. 7b's line profiles illustrate the surface parameters for two-dimensional movement. Fig. 7d shows the roughness parameters ($R_a$, $R_q$, $R_{sk}$, and $R_{ku}$).

By deducting the average roughness values in the horizontal and vertical directions, the average Ra (Surface Roughness) measurement for CLP would be 31.054 μm, as predicted. Likewise, the anticipated mean Rq (Root Mean Square Surface Roughness) value for CLP was 44.326 μm. The symmetrical arrangement of the surface profiles and the arrangement of spikes above and below the mean

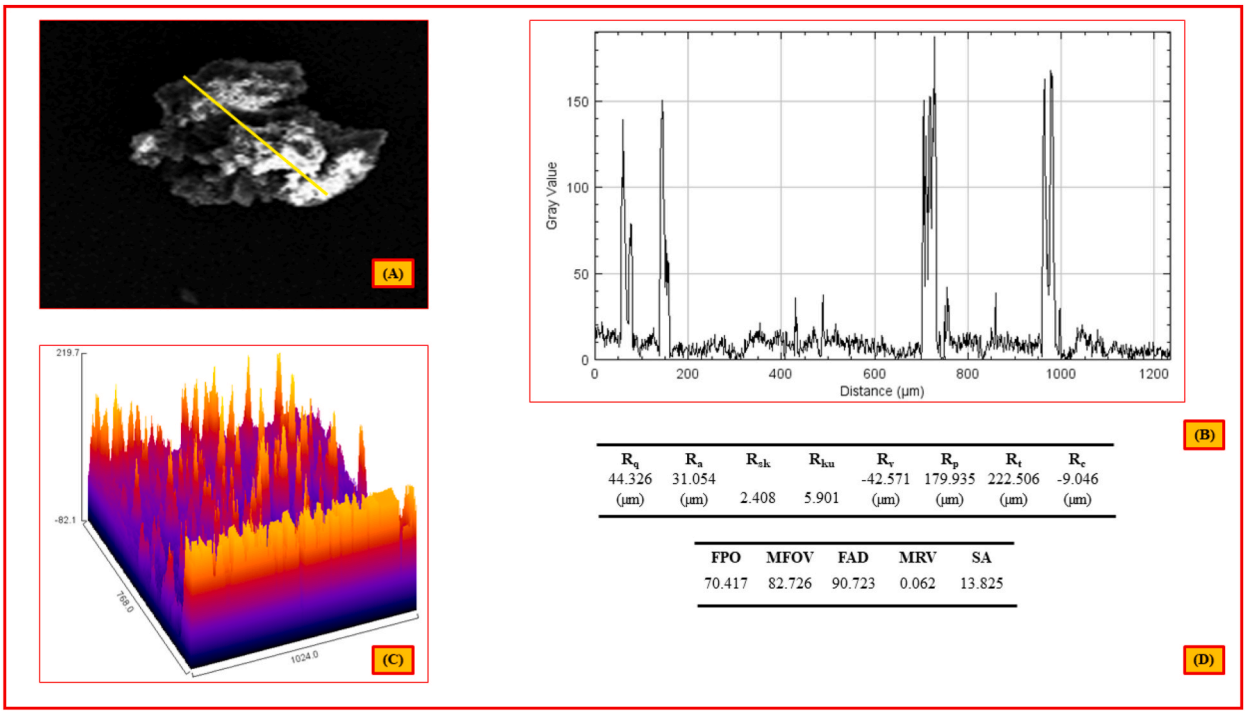


| $R_q$ | $R_a$ | $R_{sk}$ | $R_{ku}$ | $R_v$ | $R_p$ | $R_t$ | $R_c$ |
|---|---|---|---|---|---|---|---|
| 44.326 (μm) | 31.054 (μm) | 2.408 | 5.901 | -42.571 (μm) | 179.935 (μm) | 222.506 (μm) | -9.046 (μm) |

| FPO | MFOV | FAD | MRV | SA |
|---|---|---|---|---|
| 70.417 | 82.726 | 90.723 | 0.062 | 13.825 |

**Fig. 7.** (a–d) AFM analysis of ***Calotropis gigantiea*** plasticizer.

line, are described by the coefficient of kurtosis ($R_{ku}$) and surface skewness ($R_{sk}$) values respectively. The skew profile dictates the surfaces' porosity and load capacity. The skewness value of 2.408 was discovered during the current research. Because of their spiky nature, the values (5.901) in the current study are $R_{ku}>3$, which is comparable to how $R_{ku}$ values are used to define the surfaces' spiky nature. Furthermore, the SEM observations have been quantitatively corroborated by our work. As a result, it was discovered that the extracted bio-plasticizer material may be used to create biofilm and bio-composites. Therefore, the suggestion that a CLP with a rough surface is supported by the previous result.

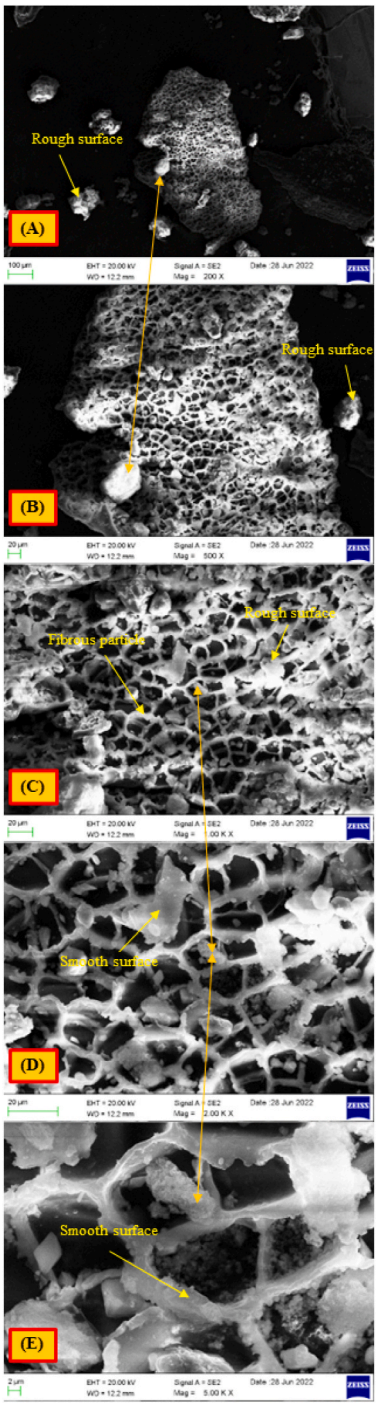


**Fig. 8.** (a–e) Scanning electron microscopic pictures of *Calotropis gigantiea* plasticizer at different magnification.

### 4.6. Morphological investigation of the surface area

#### 4.6.1. SEM topography of CLP

The SEM microphotographs of the CLP plasticizers at various magnifications, such as 200×, 500×, 1000×, 2000×, and 5000×, are displayed in Fig. 8a-e. This investigation is very important because it tells us whether the material is appropriate to utilise as a reinforcing agent in a given composite application or not. Fig. 8a's image displays a heterogeneous distribution of particles with varying sizes and shapes, but no CLP agglomerates are visible on the plasticizer's surface, suggesting that it may provide good interfacial interaction with other polymer matrices. The same observation has been reported by researchers [50]. The rough surface is shown clearly in Fig. 8b. Their form implies that the plasticizer units are composed of uneven, tiny fragments. Also, the surface of every particle is rough which gives the substrates of bio-films and bio-composite materials better reinforcing capabilities. Due to a lack of accumulation, it increases the active site for the surface area of the particles may grow due to the interaction among the plasticizer and polymer. Every image of the fracture or flakes-like surface showed gaps and cavities; this indicates that the fracture surface is brittle and has a reduced toughness. A closer look at the image in Fig. 8d reveals fine, dark micropores with a rough, uneven surface and white colour fibre with a smooth surface that is easily visible. This could be because the image contains white layers that appear to be hemicellulose and wax-like materials. The white surface showed evidence of porous sections, confirming the plasticizer's semi-crystalline structure. The results of the XRD provide evidence for this. The surface of the CLP was seen to have tiny voids and

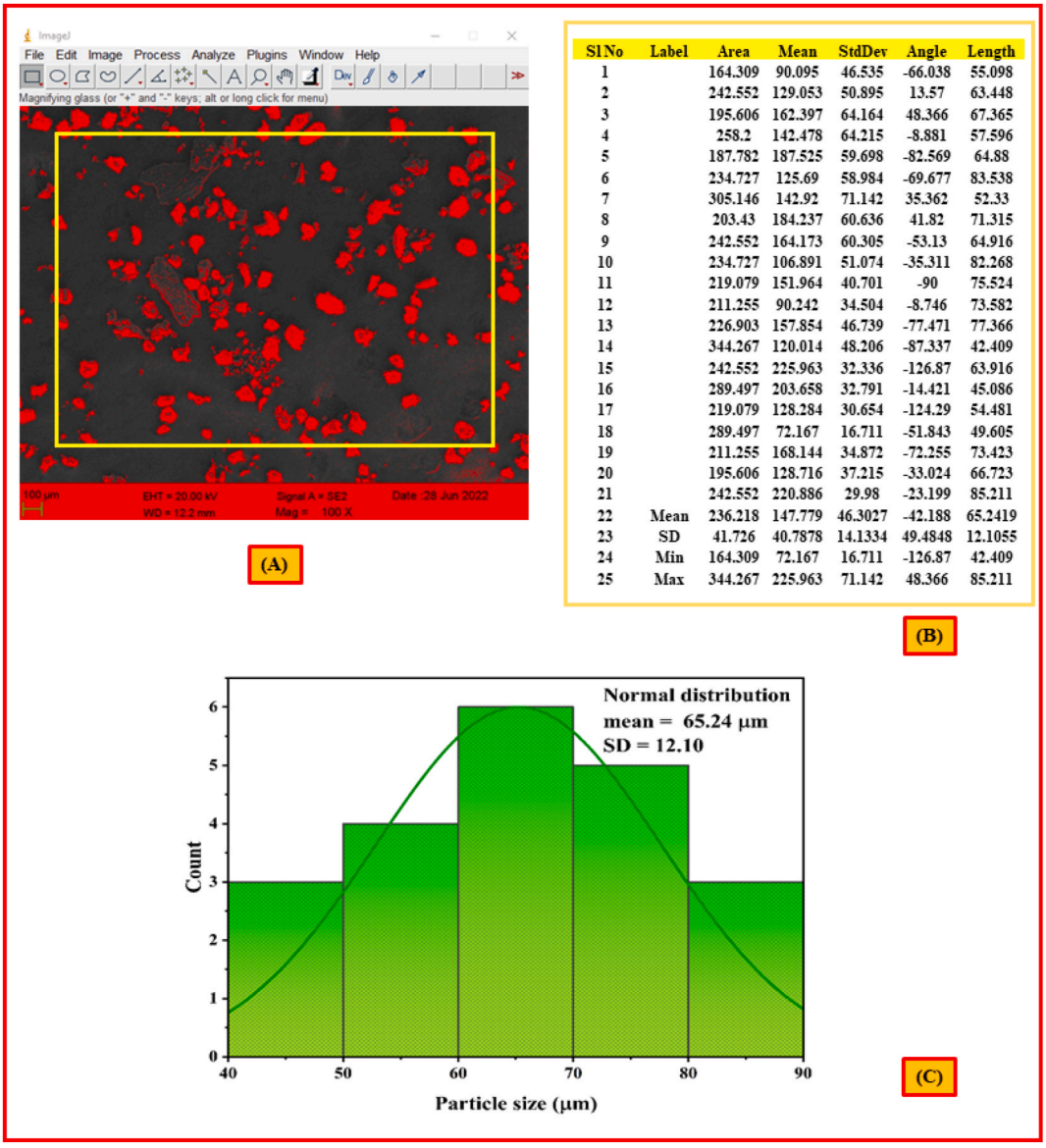


| Sl No | Label | Area | Mean | StdDev | Angle | Length |
|---|---|---|---|---|---|---|
| 1 | | 164.309 | 90.095 | 46.535 | -66.038 | 55.098 |
| 2 | | 242.552 | 129.053 | 50.895 | 13.57 | 63.448 |
| 3 | | 195.606 | 162.397 | 64.164 | 48.366 | 67.365 |
| 4 | | 258.2 | 142.478 | 64.215 | -8.881 | 57.596 |
| 5 | | 187.782 | 187.525 | 59.698 | -82.569 | 64.88 |
| 6 | | 234.727 | 125.69 | 58.984 | -69.677 | 83.538 |
| 7 | | 305.146 | 142.92 | 71.142 | 35.362 | 52.33 |
| 8 | | 203.43 | 184.237 | 60.636 | 41.82 | 71.315 |
| 9 | | 242.552 | 164.173 | 60.305 | -53.13 | 64.916 |
| 10 | | 234.727 | 106.891 | 51.074 | -35.311 | 82.268 |
| 11 | | 219.079 | 151.964 | 40.701 | -90 | 75.524 |
| 12 | | 211.255 | 90.242 | 34.504 | -8.746 | 73.582 |
| 13 | | 226.903 | 157.854 | 46.739 | -77.471 | 77.366 |
| 14 | | 344.267 | 120.014 | 48.206 | -87.337 | 42.409 |
| 15 | | 242.552 | 225.963 | 32.336 | -126.87 | 63.916 |
| 16 | | 289.497 | 203.658 | 32.791 | -14.421 | 45.086 |
| 17 | | 219.079 | 128.284 | 30.654 | -124.29 | 54.481 |
| 18 | | 289.497 | 72.167 | 16.711 | -51.843 | 49.605 |
| 19 | | 211.255 | 168.144 | 34.872 | -72.255 | 73.423 |
| 20 | | 195.606 | 128.716 | 37.215 | -33.024 | 66.723 |
| 21 | | 242.552 | 220.886 | 29.98 | -23.199 | 85.211 |
| 22 | Mean | 236.218 | 147.779 | 46.3027 | -42.188 | 65.2419 |
| 23 | SD | 41.726 | 40.7878 | 14.1334 | 49.4848 | 12.1055 |
| 24 | Min | 164.309 | 72.167 | 16.711 | -126.87 | 42.409 |
| 25 | Max | 344.267 | 225.963 | 71.142 | 48.366 | 85.211 |

**Fig. 9.** (a–c) Particle size study of ***Calotropis gigantiea*** plasticizer.

rough cavities. The CLP's tensile strength is decreased by the holes and debris, but its surface roughness is increased, improving the CLP's interfacial adhesion to the matrix polymer. Because of its facile plastic deformation, it is recommended that we utilise this CLP as a bioplasticizer. On the cracked surface of Fig. 8e, however, a compatible phase was noted and more noticeable flakes were visible, offering good mechanical qualities. The obtained CLP's size was measured by means of ImageJ software and SEM pictures. The size of the particles might be automatically estimated with the use of ImageJ and SEM micrographs of individual particles. The mean particle size was calculated using micrometre measurements of 21 different particles. Following that, the average size of the particles was discovered to be 65.24 ± 12.10 μm.

Using monochromatic images as thresholds, one may find out how big the particles are in the segmented image. Fig. 9a demonstrates the threshold collection of distinct reddish-orange microplasticizer particulates. Fig. 9b displays the data (average and standard deviation measurements) for the particle size of the plasticizer. Particle size (μm) versus count size distribution analysis is as seen in Fig. 9c's histogram plots. 60 μm–70 μm particles make up 29 % of the plasticizer, with the remainder particles consisting of 40 μm and 50 μm (14 %), 50 μm and 60 μm (19 %), 70 μm and 80 μm (24 %), and 80 μm and 90 μm (14 %), respectively. The size of plasticizer is 65.24 μm on average, with a 12.10 μm standard deviation.

### 4.7. Energy dispersive spectroscopy analysis

The highest resolution particle exterior characteristics and elemental composition fingerprints of the material were obtained by SEM/EDS. In Fig. 10(a and b), the distribution of chemical components of CLP's surface is presented in respect to weight & atomic percentage. The prominent peaks areas of carbon and oxygen were visible. The CLP also specifies minimal values for salt (14.48 wt percent) and chlorine (17.19 wt percent). Due to the higher non-cellulosic material content or from the salts employed during preparation of CLP. But when carbon and oxygen were found to be the main components, the percentage of carbon and oxygen was found to be (37.57 & 30.76 wt%), indicating that the CLP is organic in origin. The principal constituents of the plant-based organic plasticizer are carbon & oxygen. An SEM/EDX examination revealed four components in the manufactured plasticizer that are non toxic to living beings. Its high carbon content and lack of sulfur-like impurities make it an excellent reinforcing filler for polymer matrices, which would increase the composite's thermal resistance [51].

## 5. Plasticizer analysis with PBAT

By creating a film with polybutylene adipate-*co*-terephthalate (PBAT), it was feasible to examine the plasticizing impact of CLP. The mechanical characteristics of the biofilm were assessed at 30 °C and 40 % humidity using a universal testing system (QRS-S11H, Quro). Elongation tensile modulus, tensile strength, and elongation break % were the parameters that were measured. The plasticizing impact of CLP on PBAT matrix-based biofilm was confirmed in a flexibility research study using unaided inspection and SEM morphological analysis.

### 5.1. Morphology and flexibility of bio-films

The chemical bonding between the PBAT (poly(butylene adipate-*co*-terephthalate) matrix and this particular CLP plasticizer is seen in Fig. 11. Fig. 12 displays the PBAT/CLP biofilm SEM micrographs and photographs. Significant alterations in the surface morphology of PBAT were identified by the SEM photomicrographs for the PBAT/CLP biofilm. The smooth surfaces shown in the photomicrographs of the films made of plasticizer are the consequence of the synthetic CLP plasticizer's high compatibility with PBAT. The bio-films developed for this study are displayed in Fig. 12 (a & b) and Fig. 12 (c & d) also demonstrates the films' extent of flexibility.

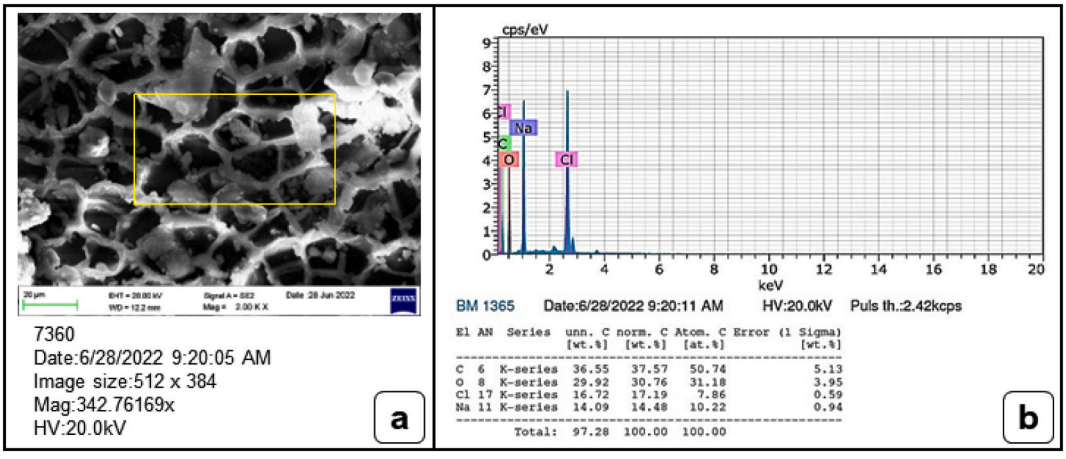


**Fig. 10.** (a & b) EDS analysis of CLP.

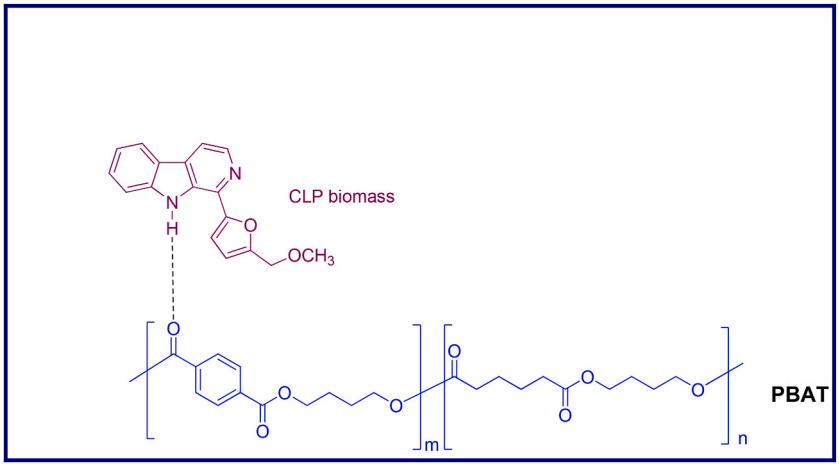


**Fig. 11.** The plasticization effect of CLP plasticizer in PBAT matrix.

Because of the plasticizer reinforcement, the bio-films' visual flexibility showed that the PBAT/2 % CLP based film appeared more flexible than the pure PBAT film. The plasticized reinforced films and pure films SEM analyses are displayed in Fig. 12 (e & f) and Fig. 12 g&h, respectively. Good connection is seen between the blends mechanical characteristics and the SEM microphotographs taken from the surface area of the samples. As seen by the black dots in the micrograph Fig. 12e, the film without plasticizer has some flaws in it. These dark patches are called micropores, and they may serve as places where microcracks grow and spread, eventually fracturing. The porous, flat surface of pure PBAT film is unfortified. There are fewer interfacial gaps on the reinforced film's outside surface than that of the pure PBAT film, making the reinforcement more noticeable. This is strongly demonstrated by the CLP fillers' good compatibility with the matrix and the polymer's sufficient reinforcement of them. But with the addition of CLP, the samples become more ductile, the surface bumps virtually vanish, and the compression-molded films look more uniform. The films that are produced have a smoother surface overall, since the low molecular weight of CLP facilitates its facile penetration and compatibilization at the biocomposite's component interface. Higher elongation at the break was the outcome of the more homogenous surface of PBAT/CLP biofilms, which also demonstrated a superior plasticizing action. The plasticizers are sporadically distributed throughout the matrix, exhibiting minimal agglomeration. For CLP/PBAT bio-film to be used on a broad scale in the future, it is advised to optimise the concentration of reinforcement.

### *5.2. PBAT/CLP bio-film tensile properties*

Tensile study of the various plasticized films was carried out in order to estimate the tensile strength, Young's modulus at different CLP concentrations, and extension at the break [52–55]. Fig. 13 illustrates how the tensile strength of PBAT film is affected by the incorporation of CLP plasticizers in varying amounts. The experiment's findings demonstrated that as the CLP concentration increased, the films tensile strength altered. The following films' tensile strengths were ascertained: 15.30 MPa, 17.15 MPa, 24.60 MPa, 21.50 MPa, 19.40 MPa, and 16.35 MPa for pure PBAT, PBAT-1 % CLP, PBAT-2 % CLP, PBAT-3 % CLP, PBAT-4 % CLP, and PBAT-5 % CLP. The tensile strength of the system containing 2 % CLP was higher than that of pure PBAT and than those with other concentrations of CLP (1 %, 3 %, 4 %, and 5 %). Fig. 14 demonstrates the relationship between the Young's modulus and different loading of CLP on PBAT. According to this investigation, the films' tensile modulus varied as the CLP concentration increased. The following films' tensile modulus were found: 137 MPa, 150 MPa, 168 MPa, 154 MPa, 147 MPa, and 140 MPa for pure PBAT, PBAT-1 % CLP, PBAT-2 % CLP, PBAT-3 % CLP, PBAT-4 % CLP, and PBAT-5 % CLP. In comparison to pure PBAT and various CLP concentrations (1 %, 3 %, 4 %, and 5 %), the addition of 2 % CLP exhibits a greater tensile modulus.

The tensile strength as well as Young's modulus of pure PBAT are 15.3 and 137 MPa, respectively. Fig. 13 illustrates a comparable pattern in the tensile strength as well. There is a decrease in the macromolecules' direct binding forces because the CLP plasticizer's molecules can pass through the interface between CLP and PBAT because of its low molecular weight. Because of this easy sliding and moving under stress, the molecular chains experience an increase in strain at breakage and a loss in stiffness. Consequently, the biocomposites' ability to plastically deform is gradually enhanced by the addition of CLP, which also lessens their stiffness-two extremely useful characteristics for the moulding and shaping operations. Consequently, the current findings unequivocally demonstrate that CLP and PBAT/CLP modified with CLP can effectively mitigate their inherent brittleness, leading to a notable enhancement of their toughness and ductility. Several investigators concurred with this finding [56,57] concerning the elastic modulus, also known as Young's modulus, which establishes a material's rigidity. In terms of the PBAT/CLP biofilm Young modulus, adding more CLP to the mixture caused the modulus to rise, which may indicate the development of composites with greater stiffness. With CLP quantities as high as 2 %, this trend was seen, and the material's Young modulus was 168 MPa. A high aspect ratio of CLP and good plasticizer dispersion in the polymer matrix promoted the hydrogen bonding and adherence between the PBAT and CLP, resulting in the production of biofilm with improved mechanical properties [38]. Interestingly, the Young modulus values of the 5 % PBAT/CLP

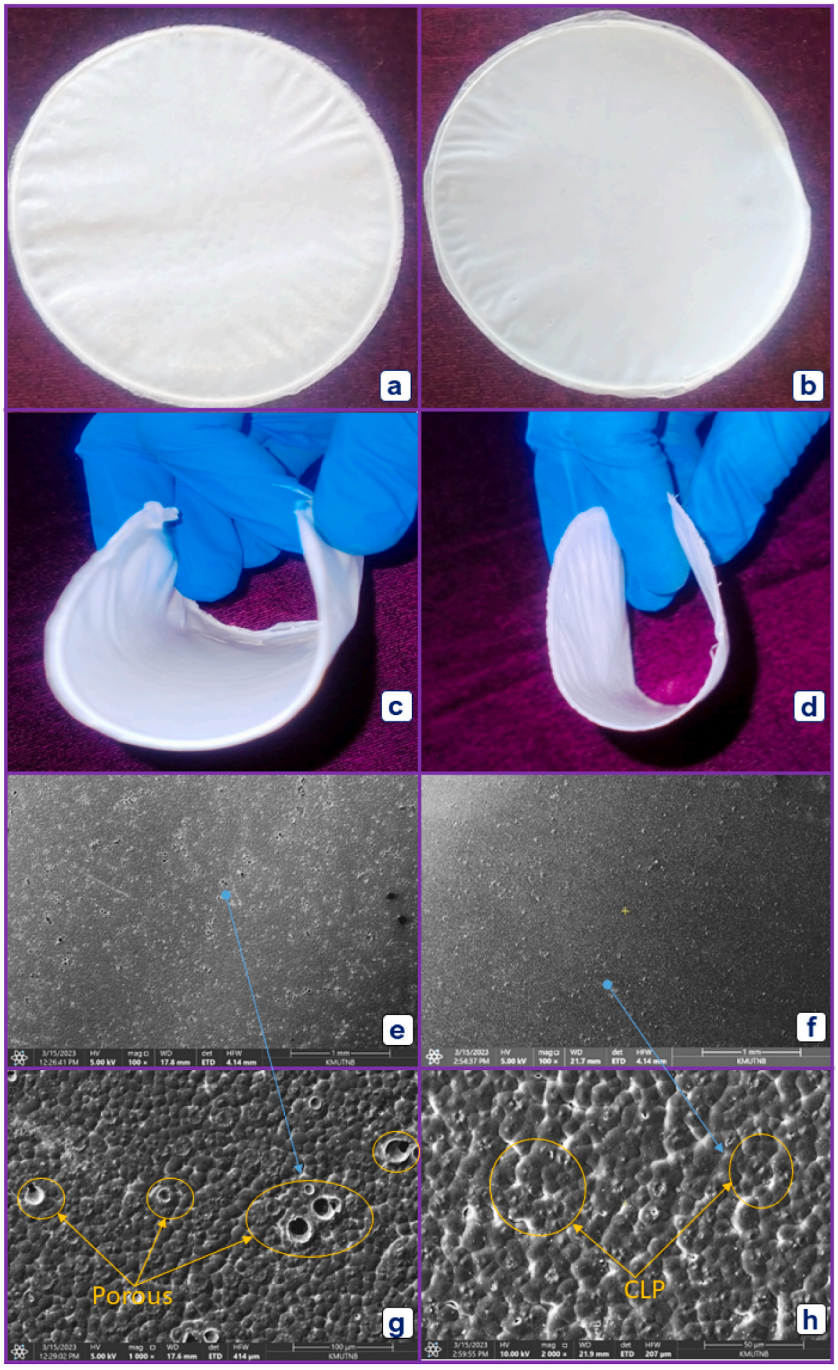


**Fig. 12.** Photo image of the biofilm enhanced with CLP plasticizer: **a** pure PBAT film; **b** PBAT/2 % reinforced biofilm with CLP plasticizer; **c** Validation of pure PBAT film's elasticity; **d** Flexibility evaluation of the biofilm reinforced with PBAT/2 % CLP plasticizer; **e**, **g** SEM images of PBAT biofilm at magnifications of 100 and 500; **f, h** SEM images of biofilm-PBAT with 2 % CLP plasticizer at 100× and 500× magnification.

combinations were almost identical to those of the pure PBAT film. Mechanical properties of PBAT/CLP are discussed in Table 2.

## 6. Conclusions

Nowadays, bio-plasticizers are gaining a lot of attention with the ultimate objective of using them to create package applications that are less detrimental to society and the environment. The solid plasticizer that was isolated from the leaves of Calotropis gigantiea was found to be an appropriate addition to biopolymer PBAT. The plasticizer was separated, and its characteristics were determined by

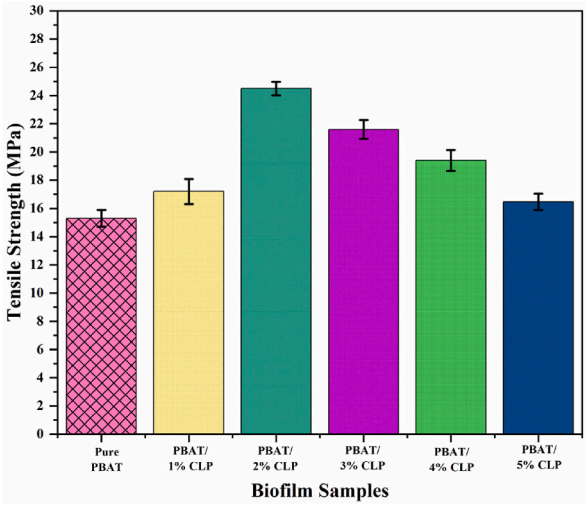


**Fig. 13.** Changes in Tensile strength of neat PBAT film and PBAT/CLP films.

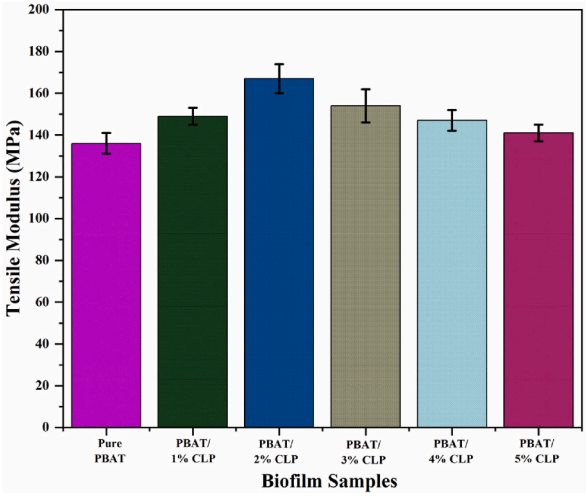


**Fig. 14.** Relationship between the Young's modulus and different loading of PBAT/CLP/biofilm.

**Table 2**
Mechanical properties of PBAT/CLP.

| Film combinations | Tensile strength (MPa) | Youngs modulus (MPa) |
|---|---|---|
| Pure PBAT | 15.30 | 137 |
| 1 % CLP | 17.15 | 150 |
| 2%CLP | 24.60 | 168 |
| 3%CLP | 21.50 | 154 |
| 4%CLP | 19.40 | 147 |
| 5%CLP | 16.35 | 140 |

FT-IR, UV–visible, X-Ray diffraction, TGA, SEM, AFM, EDX, and particle size. The rough surface of the pores on the surface of CLP is visible in the SEM pictures, and this surface is appropriate for the plasticization of novel bioplastics with strong mechanical properties. The existence of possible secondary phenolic metabolites is indicated by the presence of certain functional groups. The bio-plasticizer extracted is a promising option for lightweight biofilm application, as shown by its low crystallinity index (20.2 %), low crystalline size (5.3 nm), strong heat stability (244 °C), low density, and good surface roughness (Ra-34.154 μm). The CLP materials' amorphous structure and minuscule particle sizes (5.3 nm) promote open volume space, which contributes to an increase in plasticizer action of this new bioplasticizer was proven, according to the tensile, chemical, and morphological analysis. In order to ascertain CLP's

plasticizing capacity, pure PBAT film and CLP-enhanced biofilm was created and characterised. Compared to pure film, PBAT/CLP film exhibits greater flexibility and high surface compatibility. Young's modulus of 168 MPa and tensile strength of 24.60 MPa at 2 % CLP loading indicate that the innovative bio-flim is well-reinforced. The biofilm measured 0.8 mm in thickness. Ultimately, it has been demonstrated that the properties of CLP may suggest that it is a suitable plasticizer for addressing upcoming environmental problems with packaging materials.

## Ethical approval

Not Applicable.

## Funding

"This research budget was allocated by National Science, Research and Innovation Fund (NSRF) (Fundamental Fund 2024), and King Mongkut's University of Technology North Bangkok (Project no. KMUTNB-FF-67-B-56)."

## Availability of data and materials

The data that support the findings of this study are available on request from the corresponding author.

## CRediT authorship contribution statement

**Shanmuga Sundari Chandraraj:** Writing – original draft. **Indran Suyambulingam:** Writing – review & editing, Visualization, Supervision, Methodology, Investigation, Funding acquisition, Conceptualization. **Naushad Edayadulla:** Writing – original draft. **Divya Divakaran:** Writing – review & editing, Writing – original draft. **Manoj Kumar Singh:** Writing – review & editing. **M.R. Sanjay:** Writing – review & editing, Supervision. **Suchart Siengchin:** Writing – review & editing, Supervision.

## Declaration of competing interest

The authors declare the following financial interests/personal relationships which may be considered as potential competing interests:The Corresponding Author of this paper, Manoj Kumar Singh, works as an Associate Editor at Heliyon Materials Science. If there are other authors, they declare that they have no known competing financial interests or personal relationships that could have appeared to influence the work reported in this paper.

## Acknowledgements

This research was supported by Natural Composites Research Group Lab, Department of Materials and Production Engineering, The Sirindhorn International Thai-German School of Engineering (TGGS), King Mongkut's University of Technology North Bangkok (KMUTNB), Bangkok −10800, Thailand. In particular, the first author would like to thank Er. K. Suthakar of Rado ChemMAX in Kanyakumari, Tamil Nadu, India, for all of the support he has given during the course of this research.

## References

[1] T.D. Moshood, G. Nawanir, F. Mahmud, F. Mohamad, M.H. Ahmad, A. AbdulGhani, Sustainability of biodegradable plastics: new problem or solution to solve the global plastic pollution? Current Research in Green and Sustainable Chemistry 5 (2022) 100273 https://doi.org/10.1016/J.CRGSC.2022.100273.
[2] Y.A. Arfat, Plasticizers for biopolymer films, Glass Transition and phase transitions in food and biological materials, 159–182, https://doi.org/10.1002/9781118935682.ch6, 2017.
[3] D. Divakaran, M. Sriariyanun, I. Suyambulingam, S. Mavinkere Rangappa, S. Siengchin, Exfoliation and physico-chemical characterization of novel bioplasticizers from Nelumbo nucifera leaf for biofilm application, Heliyon 9 (2023) e22550, https://doi.org/10.1016/j.heliyon.2023.e22550.
[4] S.C. Teixeira, N.O. Gomes, T.V. de Oliveira, P. Fortes-Da-Silva, N. de F.F. Soares, P.A. Raymundo-Pereira, Review and Perspectives of sustainable, biodegradable, eco-friendly and flexible electronic devices and (Bio)sensors, Biosens. Bioelectron. X 14 (2023) 100371, https://doi.org/10.1016/J.BIOSX.2023.100371.
[5] P. Jia, H. Xia, K. Tang, Y. Zhou, Plasticizers derived from biomass resources: a short review, Polymers 10 (2018), https://doi.org/10.3390/polym10121303.
[6] M.G.A. Vieira, M.A. Da Silva, L.O. Dos Santos, M.M. Beppu, Natural-based plasticizers and biopolymer films: a review, Eur. Polym. J. 47 (2011) 254–263, https://doi.org/10.1016/j.eurpolymj.2010.12.011.
[7] M.G.A. Vieira, M.A. Da Silva, L.O. Dos Santos, M.M. Beppu, Natural-based plasticizers and biopolymer films: a review, Eur. Polym. J. 47 (2011) 254–263, https://doi.org/10.1016/J.EURPOLYMJ.2010.12.011.
[8] R.N. Darie-Niţə, C. Vasile, A. Irimia, R. Lipşa, M. Râpə, Evaluation of some eco-friendly plasticizers for PLA films processing, J. Appl. Polym. Sci. 133 (2016), https://doi.org/10.1002/app.43223.
[9] F. Ivanič, D. Jochec-Mošková, I. Janigová, I. Chodák, Physical properties of starch plasticized by a mixture of plasticizers, Eur. Polym. J. 93 (2017) 843–849, https://doi.org/10.1016/j.eurpolymj.2017.04.006.
[10] M. Yang, J. Shi, Y. Xia, Effect of SiO2, PVA and glycerol concentrations on chemical and mechanical properties of alginate-based films, Int. J. Biol. Macromol. 107 (2018) 2686–2694, https://doi.org/10.1016/J.IJBIOMAC.2017.10.162.
[11] V. Tyagi, B. Bhattacharya, Role of plasticizers in bioplastics, MOJ Food Process Technol 7 (2019) 128–130, https://doi.org/10.15406/mojfpt.2019.07.00231.
[12] H. Hosney, B. Nadiem, I. Ashour, I. Mustafa, A. El-Shibiny, Epoxidized vegetable oil and bio-based materials as PVC plasticizer, J. Appl. Polym. Sci. 135 (2018) 46270, https://doi.org/10.1002/APP.46270.
[13] Q. Fu, Y. Long, Y. Gao, Y. Ling, H. Qian, F. Wang, X. Zhu, Synthesis and properties of castor oil based plasticizers, RSC Adv. 9 (2019) 10049–10057, https://doi.org/10.1039/C8RA10288K.

[14] H. Xu, T. Fan, N. Ye, W. Wu, D. Huang, D. Wang, Z. Wang, L. Zhang, Plasticization effect of bio-based plasticizers from soybean oil for tire tread rubber, Polymers 12 (2020), https://doi.org/10.3390/POLYM12030623.
[15] A. Shafqat, N. Al-Zaqri, A. Tahir, A. Alsalme, Synthesis and characterization of starch based bioplatics using varying plant-based ingredients, plasticizers and natural fillers, Saudi J. Biol. Sci. 28 (2021) 1739–1749, https://doi.org/10.1016/J.SJBS.2020.12.015.
[16] P. Veiga-Santos, L.M. Oliveira, M.P. Cereda, A.R.P. Scamparini, Sucrose and inverted sugar as plasticizer. Effect on cassava starch–gelatin film mechanical properties, hydrophilicity and water activity, Food Chem. 103 (2007) 255–262, https://doi.org/10.1016/J.FOODCHEM.2006.07.048.
[17] D. Yun, J. Liu, Recent advances on the development of food packaging films based on citrus processing wastes: a review, Journal of Agriculture and Food Research 9 (2022) 100316, https://doi.org/10.1016/J.JAFR.2022.100316.
[18] L. Lenzi, M. Degli Esposti, S. Braccini, C. Siracusa, F. Quartinello, G.M. Guebitz, D. Puppi, D. Morselli, P. Fabbri, Further step in the transition from conventional plasticizers to versatile bioplasticizers obtained by the valorization of levulinic acid and glycerol, ACS Sustain. Chem. Eng. 11 (2023) 9455–9469, https://doi.org/10.1021/ACSSUSCHEMENG.3C01536/SUPPL_FILE/SC3C01536_SI_001.PDF.
[19] M. Kadiyala, S. Ponnusankar, K. Elango, Calotropis gigantiea (L.) R. Br (Apocynaceae): a phytochemical and pharmacological review, J. Ethnopharmacol. 150 (2013) 32–50, https://doi.org/10.1016/J.JEP.2013.08.045.
[20] C. Agyare, Y.D. Boakye, E.O. Bekoe, A. Hensel, S.O. Dapaah, T. Appiah, Review: african medicinal plants with wound healing properties, J. Ethnopharmacol. 177 (2016) 85–100, https://doi.org/10.1016/J.JEP.2015.11.008.
[21] S. Sivapalan, S. Dharmalingam, V. Venkatesan, M. Angappan, V. Ashokkumar, Phytochemical analysis, anti-inflammatory, antioxidant activity of Calotropis gigantea and its therapeutic applications, J. Ethnopharmacol. 303 (2023) 115963, https://doi.org/10.1016/J.JEP.2022.115963.
[22] G. Feng, Y. Ma, M. Zhang, P. Jia, C. Liu, Y. Zhou, Synthesis of bio-base plasticizer using waste cooking oil and its performance testing in soft poly(vinyl chloride) films, Journal of Bioresources and Bioproducts 4 (2019) 99–110, https://doi.org/10.21967/JBB.V4I2.214.
[23] J. Huang, Q. Guo, R. Zhu, Y. Liu, F. Xu, X. Zhang, Facile fabrication of transparent lignin sphere/PVA nanocomposite films with excellent UV-shielding and high strength performance, Int. J. Biol. Macromol. 189 (2021) 635–640, https://doi.org/10.1016/J.IJBIOMAC.2021.08.167.
[24] J. Chen, M. Zheng, K.B. Tan, J. Lin, M. Chen, Y. Zhu, Polyvinyl alcohol/xanthan gum composite film with excellent food packaging, storage and biodegradation capability as potential environmentally-friendly alternative to commercial plastic bag, Int. J. Biol. Macromol. 212 (2022) 402–411, https://doi.org/10.1016/J.IJBIOMAC.2022.05.119.
[25] P. Manimaran, G.P. Pillai, V. Vignesh, M. Prithiviraj, Characterization of natural cellulosic fibers from Nendran Banana Peduncle plants, Int. J. Biol. Macromol. 162 (2020) 1807–1815, https://doi.org/10.1016/J.IJBIOMAC.2020.08.111.
[26] A.A.M. Moshi, D. Ravindran, S.R.S. Bharathi, S. Indran, S.S. Saravanakumar, Y. Liu, Characterization of a new cellulosic natural fiber extracted from the root of Ficus religiosa tree, Int. J. Biol. Macromol. 142 (2020) 212–221, https://doi.org/10.1016/J.IJBIOMAC.2019.09.094.
[27] R. Md Salim, J. Asik, M.S. Sarjadi, Chemical functional groups of extractives, cellulose and lignin extracted from native Leucaena leucocephala bark, Wood Sci. Technol. 55 (2021) 295–313, https://doi.org/10.1007/S00226-020-01258-2.
[28] J.A. Okolie, S. Nanda, A.K. Dalai, J.A. Kozinski, Chemistry and specialty industrial applications of lignocellulosic biomass, Waste and Biomass Valorization 12 (2021) 2145–2169, https://doi.org/10.1007/S12649-020-01123-0.
[29] N. Izzati Ali, S. Norzahirah Zaharuddin, N. Aida Syarmeen Mohammad Azis, N. Syuhada Mohd Rafi, S. Zafirah Zainal Abidin, Conductivity and morphological studies of poly(vinyl alcohol)-magnesium triflate-ethylene carbonate gel polymer electrolyte, Scientific Research Journal 18 (2021) 161–175, https://doi.org/10.24191/srj.v18i2.13041.
[30] D. Divakaran, M. Sriariyanun, I. Suyambulingam, S. Mavinkere Rangappa, S. Siengchin, Exfoliation and physico-chemical characterization of novel bioplasticizers from Nelumbo nucifera leaf for biofilm application, Heliyon 9 (2023) e22550, https://doi.org/10.1016/J.HELIYON.2023.E22550.
[31] M.A. Ramlli, M.A. Maksud, M.I.N. Isa, Characterization of polyethylene glycol plasticized carboxymethyl cellulose-ammonium fluoride solid biopolymer electrolytes, AIP Conf. Proc. 1826 (2017) 20001, https://doi.org/10.1063/1.4979217/695209.
[32] H. Somashekarappa, Y. Prakash, K. Hemalatha, T. Demappa, R. Somashekar, Preparation and characterization of HPMC/PVP blend films plasticized with sorbitol, Indian Journal of Materials Science 2013 (2013) 1–7, https://doi.org/10.1155/2013/307514.
[33] Y. Wu, R. Tang, A. Guo, X. Tao, Y. Hu, X. Sheng, P. Qu, S. Wang, J. Li, F. Li, Enhancing Starch−Based packaging materials: optimization of plasticizers and process parameters, Materials (2023) 5953, https://doi.org/10.3390/MA16175953, 16, Page 5953 16 (2023).
[34] M.K. Mosharaf, M.Z.H. Tanvir, M.M. Haque, M.A. Haque, M.A.A. Khan, A.H. Molla, M.Z. Alam, M.S. Islam, M.R. Talukder, Metal-adapted bacteria isolated from wastewaters produce biofilms by expressing proteinaceous curli fimbriae and cellulose nanofibers, Front. Microbiol. 9 (2018) 365120, https://doi.org/10.3389/FMICB.2018.01334.
[35] D. Ray, P. Roy, S. Sengupta, S.P. Sengupta, A.K. Mohanty, M. Misra, A study of dynamic mechanical and thermal behavior of starch/poly(vinylalcohol) based films, J. Polym. Environ. 17 (2009) 49–55, https://doi.org/10.1007/S10924-009-0116-0.
[36] M.R. Amin, M.A. Chowdhury, M.A. Kowser, Characterization and performance analysis of composite bioplastics synthesized using titanium dioxide nanoparticles with corn starch, Heliyon 5 (2019) e02009, https://doi.org/10.1016/J.HELIYON.2019.E02009.
[37] J. Junthip, N. Chaipalee, Y. Sangsorn, C. Maspornpat, J. Jitcharoen, S. Limrungruengrat, T. Chotchuangchutchaval, E. Martwong, N. Sukhawipat, The use of new waste-based plasticizer made from modified used palm oil for non-glutinous thermoplastic starch foam, Polymers 14 (2022) 3997, https://doi.org/10.3390/POLYM14193997/S1.
[38] V.C. Teles, M. Roldi, S.M. Luz, W.R. Santos, L. Andreani, L.F. Valadares, Obtaining plasticized starch and microfibrillated cellulose from oil palm empty fruit bunches: preparation and properties of the pure materials and their composites, Bioresources 16 (2021) 3746–3759, https://doi.org/10.15376/BIORES.16.2.3746-3759.
[39] M.I.J. Ibrahim, S.M. Sapuan, E.S. Zainudin, M.Y.M. Zuhri, Physical, thermal, morphological, and tensile properties of cornstarch-based films as affected by different plasticizers, Int. J. Food Prop. 22 (2019) 925–941, https://doi.org/10.1080/10942912.2019.1618324.
[40] E. Zaidar, S. Lenny, S.A. Amaturrahim, S.A. Situmorang, J.N. Sari, S.U. Rahayu, S. Gea, Green plastics based on thermoplastic starch and steam-exploded nanofiber cellulose, Rasayan J. Chem 14 (2021) 1281–1288, https://doi.org/10.31788/RJC.2021.1425929.
[41] S. Nigam, A.K. Das, M.K. Patidar, Synthesis, characterization and biodegradation of bioplastic films produced from Parthenium hysterophorus by incorporating a plasticizer (PEG600), Environmental Challenges 5 (2021) 100280, https://doi.org/10.1016/J.ENVC.2021.100280.
[42] N.E. Wahyuningtiyas, H. Suryanto, E. Rudiyanto, S. Sukarni, P. Puspitasari, Thermogravimetric and kinetic analysis of cassava starch based bioplastic, Journal of Mechanical Engineering Science and Technology (JMEST) 1 (2017) 69–77, https://doi.org/10.17977/UM016V1I22017P069.
[43] B. Bouchoul, M.T. Benaniba, V. Massardier, Thermal and mechanical properties of bio-based plasticizers mixtures on poly (vinyl chloride), Polimeros 27 (2017) 237–246, https://doi.org/10.1590/0104-1428.14216/PDF/POLIMEROS-27-3-237.PDF.
[44] S.X. Tan, H.C. Ong, A. Andriyana, S. Lim, Y.L. Pang, F. Kusumo, G.C. Ngoh, Characterization and parametric study on mechanical properties enhancement in biodegradable chitosan-reinforced starch-based bioplastic film, Polymers 14 (2022) 278, https://doi.org/10.3390/POLYM14020278. , Page 278 14 (2022).
[45] P.Y. Jia, G.D. Feng, Y. Hu, Y.H. Zhou, Synthesis and evaluation of a novel N–P-containing oil-based fire-retardant plasticizer for poly(vinyl chloride), Turk. J. Chem. 40 (2016) 65–75, https://doi.org/10.3906/kim-1503-2.
[46] M.M. Rahman, S. Afrin, P. Haque, Characterization of crystalline cellulose of jute reinforced poly (vinyl alcohol) (PVA) biocomposite film for potential biomedical applications, Progress in Biomaterials 3 (2014) 1–9, https://doi.org/10.1007/S40204-014-0023-X.
[47] J. Tarique, S.M. Sapuan, A. Khalina, Effect of glycerol plasticizer loading on the physical, mechanical, thermal, and barrier properties of arrowroot (Maranta arundinacea) starch biopolymers, Sci. Rep. (2021) 1–17, https://doi.org/10.1038/s41598-021-93094-y, 11:1 11 (2021).
[48] S.B. Mhaske, N.P. Argade, The chemistry of recently isolated naturally occurring quinazolinone alkaloids, Tetrahedron 62 (2006) 9787–9826, https://doi.org/10.1016/J.TET.2006.07.098.
[49] Y. Xu, S. Wang, J. Chang, Z. Xu, Q. Zeng, Z. Wang, J. Yan, Y. Chen, A simple approach with scale-up potential towards intrinsically flame-retardant bio-based co-plasticizer for PVC artificial materials, Journal of Leather Science and Engineering 2 (2020) 1–9, https://doi.org/10.1186/S42825-020-00022-3.

[50] B.F.A. Valente, A. Karamysheva, A.J.D. Silvestre, C.P. Neto, C. Vilela, C.S.R. Freire, Epoxidized linseed oil as a plasticizer for All-Cellulose Composites based on cellulose acetate butyrate and micronized pulp fibers, Ind. Crop. Prod. 202 (2023) 116980, https://doi.org/10.1016/J.INDCROP.2023.116980.
[51] J. Intapun, T. Rungruang, S. Suchat, B. Cherdchim, S. Hiziroglu, The characteristics of natural rubber composites with klason lignin as a green reinforcing filler: thermal stability, mechanical and dynamical properties, Polymers 13 (2021) 1109, https://doi.org/10.3390/POLYM13071109. , Page 1109 13 (2021).
[52] J. Jenix Rino, I. Suyambulingam, D. Divakaran, N.P. Sunesh, M.K. Singh, M. Vishnuvarthanan, M.R. Sanjay, S. Siengchin, Facile exfoliation and physicochemical characterization of Thespesia populnea plant leaves based bioplasticizers macromolecules reinforced with polylactic acid biofilms for packaging applications, Int. J. Biol. Macromol. (2024) 129771, https://doi.org/10.1016/j.ijbiomac.2024.129771.
[53] D. Divakaran, I. Suyambulingam, M.R. Sanjay, V. Raghunathan, V. Ayyappan, International Journal of Biological Macromolecules Isolation and characterization of microcrystalline cellulose from an agro-waste tamarind (Tamarindus indica) seeds and its suitability investigation for biofilm formulation, Int. J. Biol. Macromol. 254 (2024) 127687, https://doi.org/10.1016/j.ijbiomac.2023.127687.
[54] S. Gokulkumar, I. Suyambulingam, D. Divakaran, G.S. Priyadharshini, M. Aravindh, J. Iyyadurai, M.S. Edwards, S. Siengchin, Facile exfoliation and physicochemical characterization of biomass-based cellulose derived from Lantana aculeata leaves for sustainable environment, Macromol. Res. (2023), https://doi.org/10.1007/s13233-023-00197-8.
[55] S. Boominathan, I. Suyambulingam, S. Narayanaperumal, D. Divakaran, P. Senthamaraikannan, S. Siengchin, Comprehensive characterization of novel bioplasticizer from Pandanus tectorius leaves: a sustainable biomaterial for biofilm applications, Macromol. Res. (2023), https://doi.org/10.1007/s13233-023-00192-z.
[56] K. Nanthakumar, C.M. Yeng, K.S. Chun, Tensile and water absorption properties of solvent cast biofilms of sugarcane leaves fibre-filled poly(lactic) acid, J. Thermoplast. Compos. Mater. 33 (2018) 289–304, https://doi.org/10.1177/0892705718805526.
[57] W.A. Laftah, R.A. Majid, Development of bio-composite film based on high density polyethylene and oil palm mesocarp fibre, SN Appl. Sci. 1 (2019) 1–7, https://doi.org/10.1007/S42452-019-1402-7.